(n,p) Reaction for Gold*

R. A. Peck, Jr.
Department of Physics, Brown University, Providence, Rhode Island
(Received June 11, 1956; revised manuscript received February 20, 1957)

The paper reports an experimental study of the process $Au^{197}(n,p)Pt^{197}$ induced by 14-Mev neutrons, detecting protons in the angular range 10° to 45° with emulsions. Resolution is not adequate for the identification of single excited states, but the energy spectrum does display definite structure and five groups are distinguished, chiefly on the basis of gross differences in their angular distributions. The energy widths of these groups are smaller than expected in view of the target thickness. Positions of angular distribution peaks are utilized for the assignment of angular momentum changes. The corresponding excitations in Pt^{197}, with "final angular momentum" parameters and total cross sections, are: 0.2 Mev, 2, 8.6 mb; 1.6 Mev, 0 (or 4), 2.2 mb; 2.9 Mev, 5, 2.0 mb; 4.4 Mev, 6, 5.2 mb; 6.0 Mev, 4 (or 0), 2.5 mb. The sum of these cross sections (20.5 mb) is the experimental value for the reaction cross section, since the ground state transition was probably not observed (cross section estimated not over 0.6 mb) and no significant yield of protons was observed corresponding to Pt excitation between the highest listed and the maximum (13 Mev) represented in the spectrum. All cross sections are subject to about 40% uncertainty in neutron flux, but statistical uncertainties are of order 20% or less. Maximum differential cross sections for the groups, and their locations in the angular distributions, are tabulated.

THE reaction $Au^{197}(n,p)Pt^{197}$ has been investigated with 14-Mev neutrons using photographic plates. The target material was selected for experimental convenience, the purpose of the work being to evaluate the feasibility of such studies with available neutron flux, when the cross section is of the low order typical of heavy nuclei. The results show the technique to be suitable, although resolution in the proton energy spectrum is severely limited by the thick target employed.

TECHNIQUES

Neutrons were provided by the D+T reaction, employing deuterons of 175 kev in an rf Cockcroft-Walton accelerator.[1] The tritium target consisted of 7.5 curies adsorbed in a 2-mil zirconium foil (atomic ratio roughly 1:4) and was bombarded with a steady beam of about 3.5 ma of deuterons. Neutron production was 6×10^8 neutrons/sec ma or about 60% of the yield obtained from the same tritium target when freshly cleaned. The energy spectrum of these neutrons observed at 90° to the deuteron beam is shown in Fig. 1. The main group (13 Mev and above) contains 59% of the total flux and the D+D group (1 to 3 Mev) 28%. The dashed line shows the effect on the high-energy neutrons of the iron collimator described below and shown in Fig. 2. Scattering in the collimator channel increases the width of the 14-Mev group from 0.6 Mev to 1.2 Mev.

The relative positions of neutron source, gold target, and detecting plates are shown in Fig. 2. Active area of the neutron source was an inch-diameter circle, foreshortened by inclination to about 0.7 inch in the vertical direction, and placed 8 inches from the gold target. The latter was a foil 4.8 mil thick, in the form of a square 2 inches on a side, and was backed by a thick lead sheet.[2] Two plates were placed with emulsions essentially normal to the gold foil, two inches from it in the horizontal direction and at the vertical level of its lower edge. Such an arrangement has the appearance of "poor geometry" and furnishes the relatively large detection efficiency common to this category. It is not restricted to poor geometry resolution, however, for complete microscopic measurements on each proton tract provide precise information about its spatial orientation, and so about the position in the target foil of the nucleus emitting the recorded proton. Insofar as the neutron source may be approximated by a point, the direction of neutron incidence is determined by the same information. Thus if complete measurements are made on each track the result is a set of disordered "good geometry" data. Figure 2 further shows a cylindrical iron collimator employed to reduce the primary neutron flux at the plates without increasing the tritium-to-gold distance beyond the minimum imposed by the accelerator dimension. The collimator's channel was one inch in diameter, its axis coinciding with the line joining the centers of tritium and gold films. The plates lay behind the full (5.5-inch) length of the collimator with a consequent neutron attenuation factor of order 20. One-fourth of the gold target was unshielded and the remainder lay in the "penumbra" of the collimator, shielded by a small portion of the outer rim of the channel.

The accelerator was run for 1.44 milliampere-hours with a beam intensity of roughly 3.5 ma, producing a total flux at the gold of 3.5×10^8 neutrons/cm^2 (neutrons in the 14-Mev group of the primary spectrum only). This flux was determined by recoil track density within the plates from which the proton data were taken, and

* Supported in part by the U. S. Atomic Energy Commission.
[1] R. A. Peck, Jr., and H. P. Eubank, Rev. Sci. Instr. **26**, 441, 444 (1955).

[2] The (n,p) cross section for the 52% lead isotope (208) is very small. See E. B. Paul and R. L. Clarke, Can. J. Phys. **31**, 267 (1953).

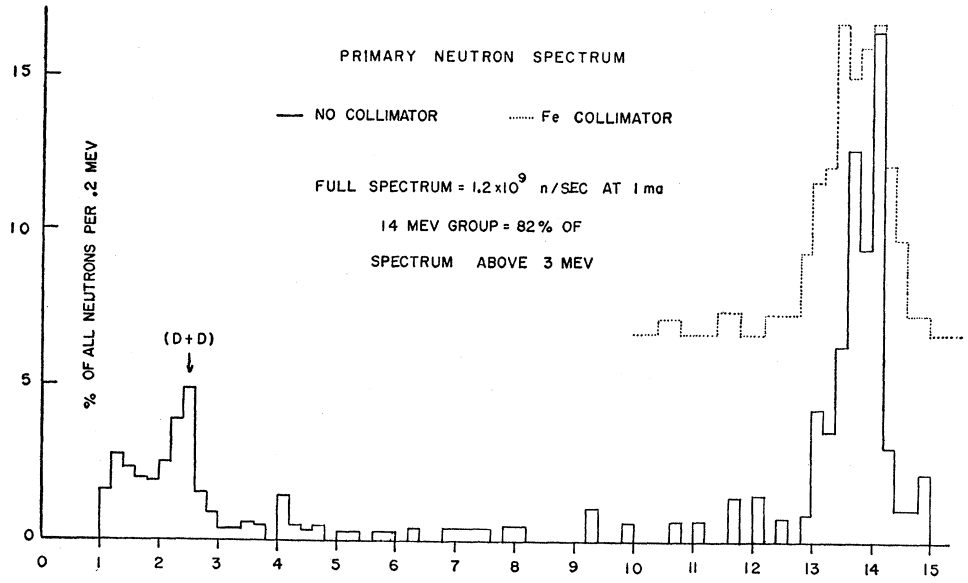

FIG. 1. Energy distribution of neutrons from the accelerator. Solid line: without collimation. Dashed line: effect of iron collimator on main group. Spectra obtained from proton recoils in Ilford C2 emulsions.

confirmed by independent measurements of the neutron production per ma-hr. Because of a time lapse between these two observations and uncertainty in the shielding effect of the iron collimator, the probable error in the neutron flux at the gold is of order 40%, although that for flux at the plates is only 8%. A similar exposure was made to evaluate experimental background effects, the background exposure being identical with the primary one except for the absence of the gold foil, an exposure 12% smaller and a slightly smaller plate area scanned.

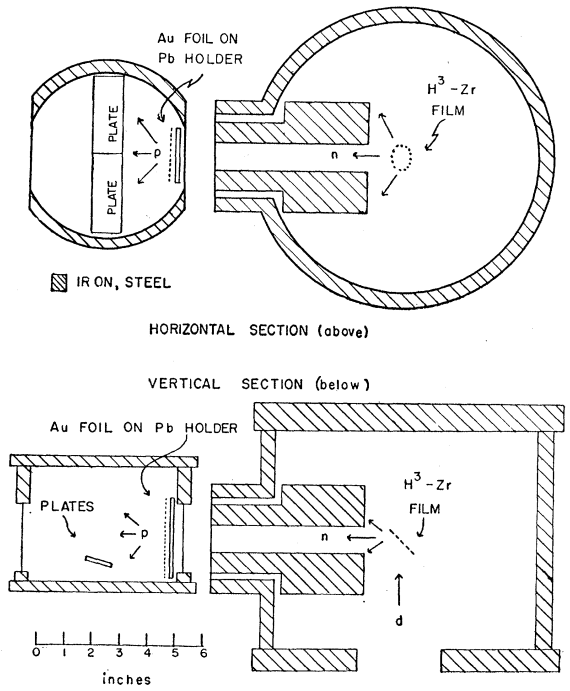

FIG. 2. Experimental arrangement.

Ilford C2 emulsions were employed, 400μ thick and on glass. They were processed by a technique varying only slightly from that of Dilworth-Stiller.[3]

Tracks were measured with a Bausch and Lomb binocular microscope employing conventional equipment and techniques. Acceptance criteria required tracks to begin at the emulsion surface and terminate within the emulsion, and to display such angles of travel (in both horizontal and vertical planes) as guaranteed their points of origin to lie within the aperture defined by the gold foil. Thus all tracks accepted must represent protons coming either from the gold or through it. To minimize discrimination errors, the observers' criteria were chosen to define a somewhat larger entrance aperture and the raw track data subjected later to a more severe discrimination. The mortality in this final discrimination was heavy. Of about 2000 incident proton tracks measured and entering from within 2° left, right and below the gold foil and roughly 10° above it, only 500 were found to come from within the gold foil. It proved absolutely necessary to employ the highest power available (1000×) and oil immersion in the surface-origin discrimination, for this system revealed as spurious roughly half of the tracks which appeared to originate at the surface under a dry objective (450×). Scanning and all other discriminations and measurements were performed with dry objective and over-all magnification of 450×. Data were obtained by three different observers (including the author), working in different areas of the plates. The data sets were analyzed separately and combined only after it was established that the three sets displayed the same general features. A similar consistency check was made of tracks origi-

[3] See J. C. Allred and A. H. Armstrong, *Laboratory Handbook of Nuclear Microscopy* [Los Alamos Scientific Laboratory Report LA-1510 (unpublished)], p. 56.

nating, respectively, in the central 25% of the gold target area and in the peripheral 75%.

Aside from identification of observer, plate, date, and chronological track number, the raw data for each acceptable track consisted of: apparent length (projection on the focal plane), angle of travel in the horizontal plane, distance of vertical travel into the emulsion, position on the plate, and local emulsion thickness. Subsequent calculations for each track yielded the angle between proton and incident neutron (the latter presumed to travel in a straight line from the center of the tritium film to the proton's point of origin in the gold foil), and the proton's full (dip-corrected) range in emulsion. Emulsion ranges were directly converted to energies using the classic calibration of Lattes, Fowler, and Cuer.[4] Although the plate housing was evacuated to eliminate proton energy loss between gold and plates, the emulsion calibration employed was that appropriate to emulsion in humidity equilibrium with the atmosphere. The energy uncertainty introduced by the slight desiccation of the plates, in vacuum for about 20 minutes, may be estimated by interpolation between the "wet emulsion" values of Lattes *et al.* and Rotblat's calibration for plates desiccated for two hours.[4] This uncertainty does not exceed 50 kev at 14 Mev and diminishes with the proton energy.

Normalization of the exposure of background plates to the primary exposure was accomplished by determinations of neutron recoil spectra in both sets of plates and comparison of track densities for both high- and low-energy groups (Fig. 1). Two observers were employed for this purpose, and the various determinations provided a normalization factor consistent within 20%. Since the background effect is small over most of the proton spectrum, this accuracy is adequate.

In consequence of the geometry of this experiment which employs extended detectors and extended proton source in close proximity, the detecting efficiency of the plates is rather strongly dependent on the n-p angle. The angular efficiency function, whose reciprocal must weight the raw yields to produce meaningful angular distributions, was determined for the particular dimensions of this experiment by numerical analysis. It is displayed in Table I, in which the angles refer to n-p space angles in the laboratory[5] and the associated numbers represent the fraction of all protons emerging from the gold target (at the associated n-p angle) which are recorded per mm^2 of emulsion area (averaged over the plate area actually scanned). The peculiar form of this angular bias is characteristic of the type of geometry employed and not an idiosyncrasy of the particular plate area scanned. The function has been computed for scanned areas of an entire plate, for 1.2 cm^2 located 0.8 cm from the end of the plate lying at the center of the chamber, and for 0.4 cm^2 located 1.8 cm from the same end. In all three cases the characteristics of the curve are qualitatively the same, nor are they very different quantitatively. In particular, the locations in n-p angle of the high and low cutoffs, of the low-angle plateau and the wide peak are the same in all cases computed. Thus the experimental arrangement is satisfactory for the study of angular distributions in the range from 10° to 45°, although its response is not constant in this range.

TABLE I. Angular efficiency function.

5°	0
10°	2.72×10^{-5}
15°	2.87×10^{-5}
20°	2.55×10^{-5}
25°	3.60×10^{-5}
30°	4.43×10^{-5}
35°	5.63×10^{-5}
40°	3.64×10^{-5}
45°	1.19×10^{-5}
50°	0.09×10^{-5}

RESULTS

The distribution in energy of acceptable proton tracks from the primary exposure (before adjustment for background yield) is shown in Fig. 3. The top graph is a conventional representation of the observed numbers of tracks falling in successive energy increments of 0.2 Mev, while the lower part presents the same data in the form of energy-density of tracks over an interval of 0.4 Mev, on the same ordinate scale as the histogram above, evaluated and plotted at closely spaced energies. The lower curve, which is an accurate representation of the points (not smoothed), is a highly redundant presentation of the data but serves to eliminate structure arising from the arbitrary location of histogram boundaries. The lower plot must of necessity eliminate all structure finer than about 0.4 Mev, but in view of the primary neutron inhomogeneity and target thickness no such structure can have significance in this experiment. Dotted lines in the lower figure show a separation of twice the probable error for the average yield in the region covered (i.e., $\bar{N}\pm0.6745\bar{N}^{\frac{1}{2}}$, where $\bar{N}$ is the mean ordinate).

Background track data were taken by two observers following exactly the same procedures as for the gross yield. Consistency was again checked before combination of the data. The background spectrum was normalized to compensate for slightly different neutron flux and scanned plate area plotted, smoothed and then subtracted from the gross yield to provide the net yield. The background spectrum was relatively unstructured, and displayed the following characteristics (intensities normalized on same scale as Fig. 3): at 14.0 Mev, a peak of maximum intensity 2 tracks/0.2 Mev and 1 Mev full width at half-maximum; from 13.5 to 9.5 Mev, a constant intensity of 1 track/0.2 Mev; from 9.5 to 4.7 Mev, a constant intensity of 0.5 track/0.2 Mev; from 4.7 to 3.0 Mev, a group with

[4] Reference 3, Appendix A.

[5] For a nucleus as heavy as gold, the center-of-mass and laboratory systems are essentially identical.

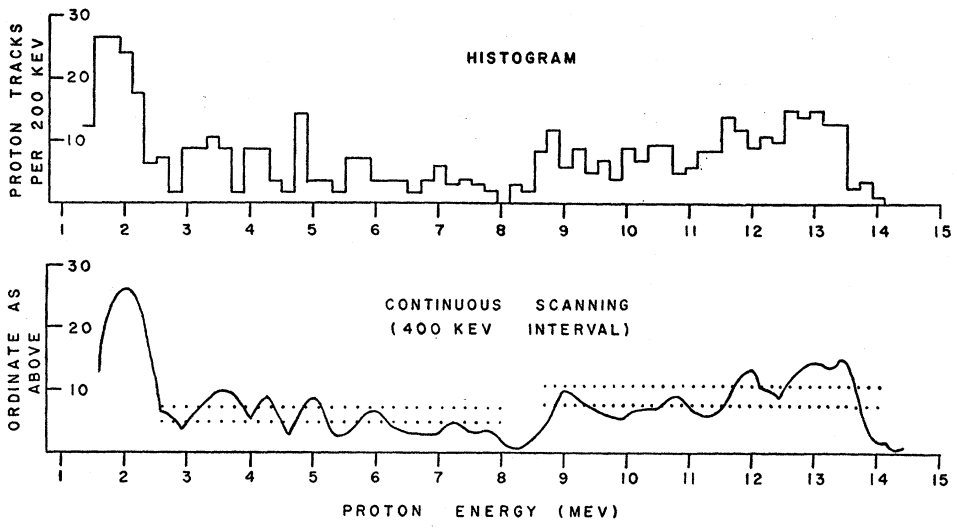

FIG. 3. Proton energy distribution (500 tracks) from the reaction $Au^{197}(n,p)Pt^{197}$. Above: histogram, 200-kev intervals. Below: 0.5×number of tracks per 400 kev, plotted continuously (redundant histogram). Dotted lines are separated by twice the probable error for mean intensity in the region covered. Gross yield is represented, before subtraction of normalized background.

peak intensity of 9 tracks/0.2 Mev at 3.7 Mev; and from 3.0 to 1.5 Mev a group with peak intensity of 18.5 tracks/0.2 Mev at 2.2 Mev. The effect of background removal is thus to eliminate the small vestige of structure at and above 14.0 Mev and also to eliminate[6] all yield in the gross spectrum below 4.7 Mev of proton energy. The background has no significant effect on the proton spectrum between 4.7 and 14.0 Mev.

The identification of bona fide energy groups with the poor resolution of this experiment is difficult, and several differential plots were employed for the purpose, including those of Fig. 3 and others with larger and smaller energy intervals. Groups may be sought only above 4.7 Mev, since below that energy no statistically significant excess of gross yield over background yield has been found. Legitimate groups may be identified in three independent ways. (a) Width. Each group should have a flat top of width equal to the target thickness (ranging from 1.7 Mev at 14 Mev to 3.4 Mev at 5 Mev) flanked by a region of decreasing intensity on each side roughly 0.6 Mev wide, the last representing the primary neutron inhomogeneity; proton straggling in the gold does not in general exceed 0.1 Mev and results only in a slight broadening of the 0.6-Mev region. On this basis one is inclined to identify only three groups, roughly 14.0 to 11.0 Mev, 11.0 to 8.2 Mev, and 8.2 to 4.7 Mev, but the identification is dubious. (b) Intensity variation. As just noted, the intensity in each group should remain constant over most of its extent, within statistical fluctuation limits. On this basis (see Fig. 3, lower) it is clear that the region between 14.0 and 8.2 Mev contains at least two groups and possibly four, and that there is no evidence for more than one group in the region from 8.25 to 5.4 Mev. (c) Angular distribution. The least ambiguous criterion whereby independent groups may be identified is the requirement that all subclasses of a single group should display the same angular variation. This fact was employed to discriminate between the alternative assignments suggested by the preceding arguments. In Fig. 4 is plotted the variation in yield (corrected for the angle-dependent recording efficiency of Table I and for the variation with angle of solid angle per degree) for the central portion of each of the possible energy groups above 8.25 Mev, and for all tracks from 5.4 to 8.25 Mev. It should be noted that although the distributions of Fig. 4 have been corrected, the same correction function has been applied to each group; the differences between the various groups are equally noticeable when the raw data are similarly distributed in angle.

There is a marked difference between the distributions for groups IA and IB (see caption, Fig. 4) and between those for IIA and IIB, whereas the distributions for two similar portions of group III have the same distribution within ± the probable error at each angle. Thus five groups are identified above 5.4 Mev rather than three. These groups are unexpectedly narrow, having roughly the same spread as the primary neutrons; the expected contribution of target thickness to width does not appear. It is clear that the groups identified cannot correspond to single levels of the residual nucleus, though they may reflect slow variations in its level density. In any case, they appear to represent significantly different portions of the energy spectrum.

Energy groups having been identified by consideration of differential energy plots, the net data (gross yield less smoothed background at each energy) were plotted as a fully integrated energy distribution. From this integrated curve the extrapolated energy[7] and total number of tracks were obtained for each group. This information appears in the first three columns of Table II.

[6] Within statistical uncertainty; the excess of gross yield in this region over background is approximately equal to the sum of the probable error in each.

[7] M. S. Livingston and H. A. Bethe, Revs. Modern Phys. **9**, 287 (1937).

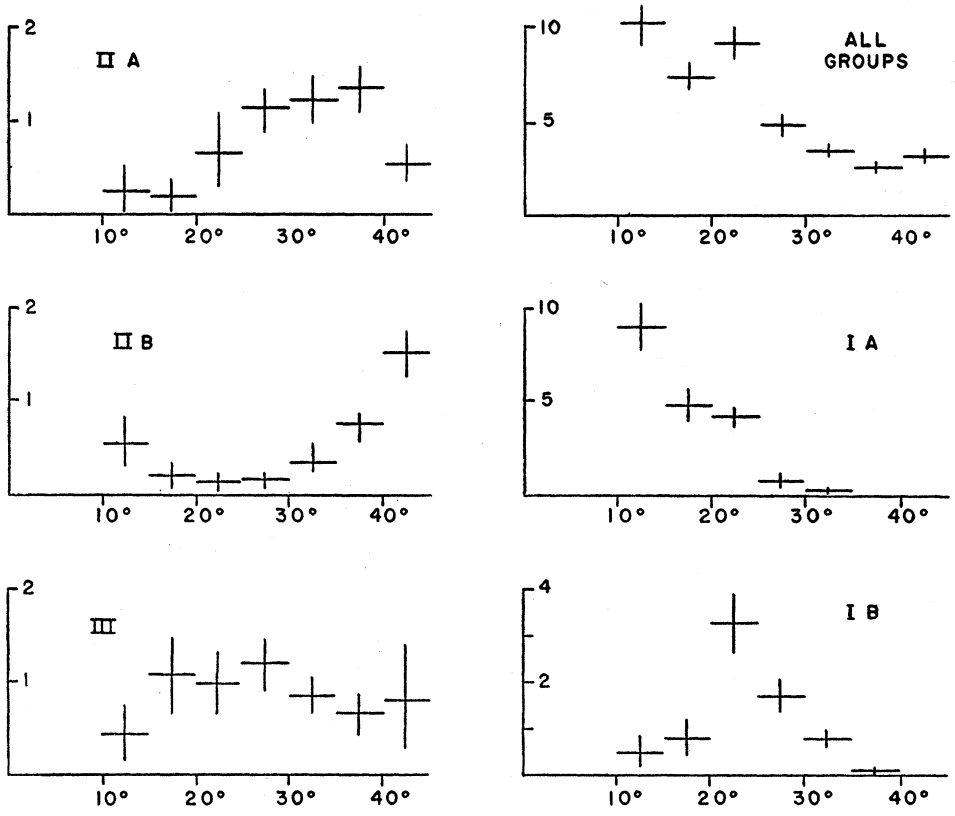

FIG. 4. Angular distributions for protons in selected energy ranges. Ordinates: millibarns per steradian (all values should be increased by 42%), vertical lines showing ± probable error based on actual track numbers. Abscissas: angle between incident neutron and emergent proton, horizontal lines showing range of angles included in the data point. Group IA: 12.6 to 13.7 Mev, 73 tracks. Group IB: 11.5 to 12.1 Mev, 33 tracks. Group IIA: 10.0 to 11.0 Mev, 38 tracks. Group IIB: 8.3 to 9.7 Mev, 44 tracks. Group III, 5.4 to 8.2 Mev, 41 tracks.

The excitation of the residual nucleus Pt^{197} corresponding to each group appears in the last column of Table II, the various proton energies (second column) being corrected for Pt recoil energy before subtraction. In computing this correction, the reaction angle corresponding to the mean of the uncorrected angular distribution was used for each group.

The maximum Q value for this reaction, corresponding to the ground state transition, may be determined from the beta-decay energy of Pt^{197} and is +0.03 Mev.[8] The Q value for the group of highest energy observed (IA, proton energy 13.95 Mev) is −0.17 Mev. The discrepancy between these values is roughly three times the combined estimated uncertainties, and is therefore considered significant. Consequently it is assumed that the ground state transition has not been observed and that the first group in the proton spectrum represents an excited state in Pt^{197}. It may be noted that some small yield does occur in the gross spectrum (Fig. 3) at the proper energy to represent the ground state transition, but that this yield is removed by subtraction of the normalized background. An upper limit to the net yield of a ground state group may be set by assuming the background correction to have been totally in error, the gross yield above 14.0 Mev then representing the ground state transition. The upper limit so determined is 10% of the intensity of group IA. It may be noted that in the reverse process, the beta decay of Pt^{197}, the direct transition to the ground state of Au^{197} is not observed.[8]

TABLE II. Groups in proton energy spectrum. Column 2 is total number of tracks in group and Column 3 extrapolated energy, both from integrated spectrum. Column 4 is corresponding Q value based on mean n-p angle for group, and Column 5 the excitation of residual Pt^{197} nucleus. Top line represents ground state transition, for which no group is observed.

Group	Yield	Energy (Mev)	Q (Mev)	Excitation (Mev)
···	Not observed	···	+0.03±0.01	0.00
IA	70	13.95	−0.17±0.05	0.20±0.06
IB	44	12.55	−1.57±0.10	1.60±0.11
IIA	43	11.26	−2.85±0.05	2.88±0.06
IIB	30	9.70	−4.41±0.10	4.44±0.11
III	48	8.09	−6.02±0.10	6.05±0.11

The angular distributions of Fig. 4 may be compared with the behavior anticipated from a direct-interaction (n,p) process[9] within the limits of the experimental resolution. In the present experiment this comparison cannot be extended to the shape of the angular distribution, but should be valid for the location of the first angular peak. It should be noted that in the region plotted, from 10° to 45°, the angular correction function (Table I) varies fairly slowly and should be reliable; the 5° region nearest to cutoff at each end has been

[8] $Q_{np}=m_nc^2-m_p^2-E=+0.78-0.75+0.03$ Mev. Data from R. W. King, Revs. Modern Phys. **26**, 378 (1954).

[9] Austern, Butler, and McManus, Phys. Rev. **92**, 350 (1953).

TABLE III. Angular distribution maxima and associated angular momentum changes. Column 4 shows location of first peak in square of spherical Bessel function of order l_{min}. Modification of the theoretical model lowers the angles in Column 4 slightly.[9] Group III may be isotropic; the assignment listed is based on the assumption that it is not.

Group	Observed peak angle	l_{min}	Calculated peak angle
IA	12.5°	0	0°
IB	23°±3°	2	25°
IIA	35°±5°	3	35°
IIB	42.5°	4	44°
III	(25°±5°)	(2)	22°

omitted. Further, the tracks plotted in each distribution should give a "pure" representation of the group since the regions in which groups appear to overlap in energy have been omitted (caption, Fig. 4). The location of the first angle peak for each group is listed in the second column of Table III, the last column showing the expected location of the first angle peak if the group is assigned the "l_{min}" value of the third column. The assignments are unambiguous, i.e., only one l_{min} value gives peak within experimental uncertainty of observed location. "Calculated peak angles" are simply those of the first peaks in the squared spherical Bessel functions of order l_{min}, of the argument QR, using $R=9.5\times10^{-13}$ cm, the value which provides best agreement between observed and expected peak locations. Q is the magnitude of the vector difference between proton and neutron wave numbers, *viz.*,

$$Q=[(k_p-k_n)^2+4k_pK_n\sin^2(\theta/2)]^{\frac{1}{2}},$$

θ being the angle between neutron and proton directions in the center-of-mass system (=laboratory angle). The k values are given for the appropriate energies E, in Mev, by $2.21\times10^{12}E^{\frac{1}{2}}$ cm^{-1}.

If the l value for the ground state of Au^{197} is known (l_p), each observed l_{min} implies an angular momentum value (l_n) for the final nucleus [Eq. (11), reference 9]. These assignments are given in the third column of Table IV, where we have assumed[10] $l_p=2$ for the ground state of Au^{197} and $l_n=1$ for the Pt^{197} ground state. Where l_n is not uniquely determined by l_{min}, the alternative listed outside of the parentheses is the one providing the better fit to the data, judged by the implied admixture of higher order Bessel functions.[9] The significance of the l_n values in Table IV is quite unclear, for it has been noted that the energy groups should not reflect transitions to isolated nuclear states such as understood in reference 9.

From observed track numbers for any group or combination, one can compute the corresponding absolute cross section from the measured neutron flux quoted earlier and the plate area scanned (117.8 mm^2). In the case of angular distributions of the several groups, (to determine the absolute ordinates of Fig. 4) the raw track numbers were multiplied by the ratio of number of tracks in the energy group (determined from the integral energy spectrum and listed in Table II) to the number of tracks in the restricted energy range selected for plotting. This ratio was within 30% of unity in all cases. The uncertainties listed (Table IV) represent probable errors based on number of tracks involved in the determination, and in all cases are to be combined with a systematic uncertainty of 39% in the neutron flux. Since flux determination with a calibrated long counter is generally good to within a few percent, the uncertainties listed are indices of the reliability of an experiment of this type, rather than the gross error of order 40%–50% which must be attached to the absolute cross sections actually obtained.

Cross sections for the several portions of the energy spectrum are presented in Table IV. The differential cross sections are the peak values occurring in the angular distributions (Fig. 4) and occur at the angles listed in Table III for the same groups. The total cross sections correspond to the total yield for each group as determined by an integration over the angular distribution for that group, extrapolated where necessary. The extrapolations involve trivial additions to yields actually observed except in the cases of group IA, extrapolated to a peak value of 15.2 mb/steradian at 0°, and group IIB, extrapolated to a peak of 2.9 mb/steradian at 45° and then doubled. The sum of the total cross sections in Table IV gives 20.5 mb for the cross section of the reaction for all groups observed, i.e., for all protons with energies exceeding 5.4 Mev. The probable error in this value, based on the number of observed tracks contributing to it, is 4%, which must be combined with the systematic uncertainty of 39% in neutron flux.

Little can be said about the cross section for protons below 5.4 Mev; while there is a finite excess in this region of gross yield over normalized background, it has already been noted that this excess is essentially equal to the sum of probable errors in gross and background values. Thus there is a chance of roughly 25% that the

TABLE IV. Cross sections and final angular momenta for the various energy groups l_n is angular momentum of Pt^{197} implied by l_{min}, alternative assignments being listed in parentheses (see text). Column 4 shows the maximum differential cross section reached in observed angular distribution and column 5 cross section based on total number of tracks in group. Uncertainties listed are probable errors (0.67 times square root of number of tracks involved) and must be combined with systematic uncertainty of 39%.

Group	Excitation (Mev)	l_n	$d\sigma/d\Omega$ (mb/sterad)	σ (mb)
Not obs.	0.00	1	...	0.85
IA	0.20±0.06	2	⩾12.7±14%	8.60±8%
IB	1.60±0.11	0(4)	4.7±20%	2.25±10%
IIA	2.88±0.06	5	2.0±19%	1.98±10%
IIB	4.44±0 11	6	>2.1±17%	5.24±12%
III	6.05±0.11	4(0) or isotropic	1.8±24%	2.46±10%

[10] P. F. A. Klinkenberg, Revs. Modern Phys. 24, 70–71 (1952), and reference 8.

difference is accidental and that no true net yield is indicated. It is not fruitful to examine the angular distribution of tracks in this region since the large background contribution cannot be separated from the gross yield. For the sake of quantifying the yield in this region, a cross section may be computed on the assumptions that the net yield observed does represent (n,p) yield and that the angular distribution is isotropic between 10° and 45°. On the basis of these assumptions the differential cross section for this low-energy portion of the spectrum is 6.6 mb/steradian.

ACKNOWLEDGMENTS

Generous assistance and helpful discussions have been provided by Professor Harold P. Eubank. Among the plate readers, the work of Mr. Robert W. Morse has been particularly helpful. The continued encouragement of the U. S. Atomic Energy Commission is acknowledged with thanks.

PHYSICAL REVIEW VOLUME 106, NUMBER 5 JUNE 1, 1957

Study of $Al^{27}(n,p)Mg^{27}$ at 14 Mev*

R. K. Haling,† R. A. Peck, Jr., and H. P. Eubank
Department of Physics, Brown University, Providence, Rhode Island

(Received November 1, 1956; revised manuscript received February 20, 1957)

Protons emerging from aluminum foil bombarded by D+T neutrons have been studied with 400 μ emulsions recording over a continuous range of angles from 15° to 165°. Groups in the composite energy spectrum correspond to known Mg^{27} levels at 1.0 and 3.5 Mev and suggest additional ones at 1.6, 5.7, and 7.0 Mev. The nuclear "temperature" for the continuous portion of the spectrum is 1.2 Mev. The following cross sections are tabulated: for each energy group, isotropic and anisotropic total cross sections and maximum differential cross section; for all protons over 2 Mev, differential cross sections at 30° intervals. The isotropic component greatly exceeds the forward-peaked one for each group. Total cross section for the reaction is estimated to be 79±15 millibarns.

INTRODUCTION

EXCITED levels of the Mg^{27} nucleus have been identified[1–3] from the reaction $Mg^{26}(d,p)Mg^{27}$ and spins assigned by reference to stripping theory,[3] as follows: ground state ($\frac{1}{2}+$), 1.0 Mev ($\frac{3}{2}+$, $\frac{5}{2}+$), and 3.5 Mev ($\frac{1}{2}+$). Studies of proton emission from the same compound nucleus in the (n,p) reaction on Al^{27} have been limited to determinations (for neutrons of 14 Mev) of the total cross section [79 mb[4] and 52.4 mb[5]] and the differential cross sections [10 mb[6] over the range 0° to 50° and 16 mb[7] at 0°]. In the experiment to be reported, nuclear emulsions have been employed to study the reaction $Al^{27}(n,p)Mg^{27}$ in detail.

EXPERIMENTAL DETAILS

Neutrons were produced by the D+T reaction initiated by 150-kev deuterons in an rf Cockcroft-Walton.[8] The source provides a neutron group of 14.1-Mev maximum energy and approximately 1-Mev width at half-maximum, at the laboratory angle (90° to the incident deuterons) employed in the experiment.

Protons were recorded in Ilford C2 emulsions 400 μ thick, placed at mean angles of 30°, 60°, 90°, 120°, and 150° to the neutron beam, and a sixth plate directly in the neutron beam was exposed simultaneously to determine neutron flux and check its energy spectrum. The emulsion planes were vertical and inclined at 15° to the direction of proton incidence from the center of the aluminum target. The target was a sheet of commercial aluminum foil mounted at 45° to the neutron beam. Nominal purity of the foil is 99.5%, the principal contaminants being iron (0.4%) and silicon (0.1%); its thickness, 4.5 mg/cm², is equivalent for protons to 200 kev at 10 Mev and 500 kev at 2 Mev.

Plates and aluminum target were enclosed in an evacuated cylindrical steel chamber 16 inches in diameter and 6 inches high. This chamber was lined with lead to reduce proton background from reactions in the walls. External shielding amounted to approximately 18 inches of iron and reduced the neutron intensity at the plates by a factor of 2000 (observed) over the unshielded value. A channel in the iron shield permitted the passage of an unobstructed neutron beam 2 inches in diameter at the aluminum target.

Total neutron flux at the aluminum was 1.5×10^9 neutrons/cm² as determined from recoil track density

* Supported in part by the U. S. Atomic Energy Commission. Submitted by R. K. H. in partial fulfillment of the requirements for the degree of Doctor of Philosophy at Brown University.

† Now at General Electric Company, San Jose, California.

[1] J. Ambrosen, Nature **169**, 408 (1952).

[2] Endt, Hafner, and Van Patter, Phys. Rev. **86**, 518 (1952).

[3] J. R. Holt and T. M. Marsham, Proc. Phys. Soc. (London) **A66**, 258 (1953).

[4] S. G. Forbes, Phys. Rev. **88**, 1309 (1952).

[5] E. B. Paul and R. L. Clarke, Can. J. Phys. **31**, 267 (1953).

[6] L. Colli and U. Facchini, *Proceedings of the International Conference on Nuclear Reactions, Amsterdam, July 2–7, 1956* (Nederlande Natuurkundige Vereniging, Amsterdam, 1956).

[7] D. L. Allan, Proc. Phys. Soc. (London) **A68**, 925 (1955).

[8] R. A. Peck, Jr., and H. P. Eubank, Rev. Sci. Instr. **26**, 441, 444 (1955).